

Electronic Supporting Information for
Stabilizing the B-site Oxidation State in ABO₃ Perovskite Nanoparticles

Tochukwu Ofoegbuna,^a Pragathi Darapaneni,^a Smriti Sahu,^a Craig Plaisance^a and James A. Dorman ^{*a}

^a Cain Department of Chemical Engineering, Louisiana State University, Baton Rouge, Louisiana 70803, United States.

* Corresponding Author

Email: jamesdorman@lsu.edu.

Experimental

Fourier-transform infrared (FTIR) spectroscopy was performed on the as-synthesized SNO (Sr/Nb=1.3) NPs using a Bruker Tensor 27 FT-IR spectrometer equipped with a DTGS detector, KBr beamsplitter, and MIRacle single reflection diamond/ZnSe attenuated total reflectance cell. The spectra were collected by averaging 128 scans in the range of 4000 to 400 cm^{-1} and with a resolution of 4 cm^{-1} .

In order to measure the Sr and Nb concentrations, a Perkins Elmer Optima 8000 inductively coupled plasma optical emission spectrometer (ICP-OES) equipped with an auto sampler was used. Samples for ICP-OES analysis were prepared by digesting 9 mg of the SNO NPs in a HNO_3 (MiliporeSigma, 65%) and HCl (VWR BDH Chemicals, 38%) solution which is heated to $\sim 90^\circ\text{C}$. Next, the digested sample is diluted to 10 ppm using 2% HNO_3 .

Iodometric titration was performed to investigate the oxygen vacancy concentration (δ) in the Sr-deficient lattice. Briefly, 9 mg of SNO (Sr/Nb=1.3) NPs were dissolved in 3 mL of 2 M KI (VWR BDH Chemicals, ACS) solution and degassed with flowing N_2 for 5 min in an Erlenmeyer flask. Next, 25 mL of 1 M HNO_3 (MiliporeSigma, 65%) was added to the mixture under vigorous stirring. 0.1 M $\text{Na}_2\text{S}_2\text{O}_3$ (Spectrum Chemical Mfg. Corp., anhydrous $\geq 97\%$), which was standardized against H_2O_2 (VWR BDH Chemicals, 3%), was titrated into the solution under inert conditions. The endpoint of the titration is detected using a starch indicator. The titration was repeated three times for the SNO sample and a blank titration (no sample) was performed to subtract atmospheric oxygen contribution.

A combination of Rietveld Refinement and O 1s XPS analysis was also utilized in calculating the δ . Rietveld refinement was performed assuming no oxygen vacancies in the Sr-deficient phase. From the deconvoluted O 1s spectrum, the peak area and ratios for the Stoichiometric and Sr-deficient lattice were extracted. The ratio extracted from the O 1s spectrum compared to the Rietveld refinement for the Sr-deficient phase was smaller due to the presence of oxygen vacancies. In order to quantify the oxygen vacancy concentration, the ratio of the O 1s spectrum was corrected using the Rietveld refinement ratios (in mol%). During the correction, the area under the Stoichiometric peak was held constant and the Sr-deficient peak area was allowed to change until the area ratio matched that of the ratio acquired from Rietveld Refinement. The increase in the Sr-deficient phase peak area is attributed to the filling of oxygen vacancy sites. For this reason, the oxygen vacancy area is the difference between the Rietveld refinement and the O 1s spectrum, and the oxygen vacancy concentration is the ratio of oxygen vacancy to oxygen in the Sr-deficient lattice.

Figures

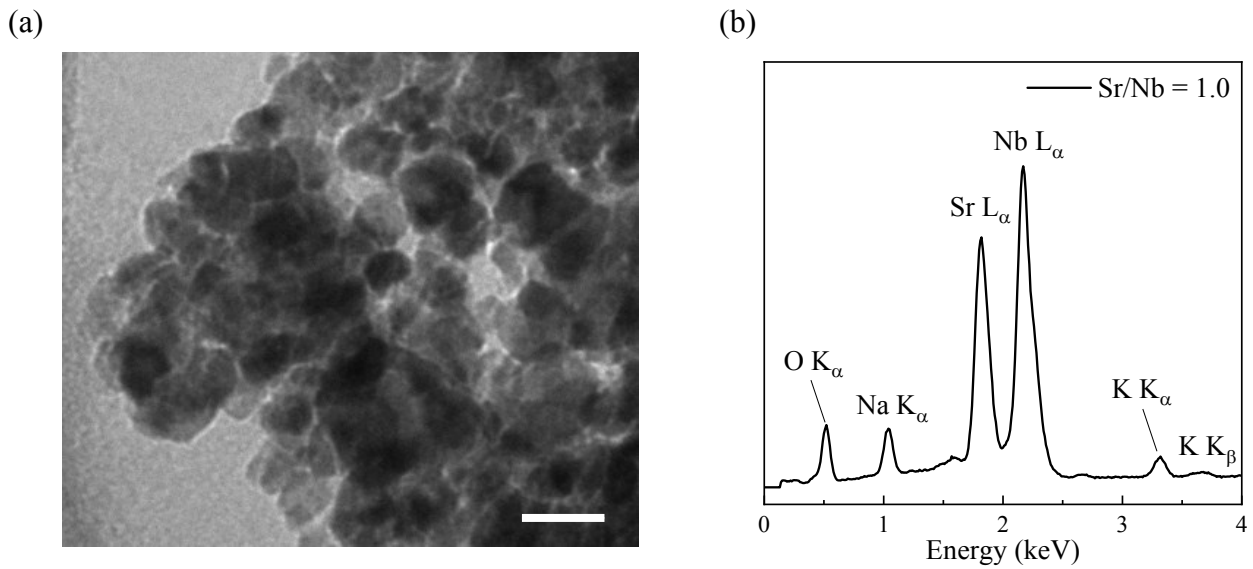


Figure S1. (a-b) TEM/ EDX of the $\text{Sr}_{1-x}\text{NbO}_{3-\delta}$ ($\text{Sr}/\text{Nb}=1.0$) nanoparticles synthesized under total pressure of 0.2 Torr. Nanoparticle sizes are approximately 10 to 20 nm. The scale bar in the TEM image is 50 nm.

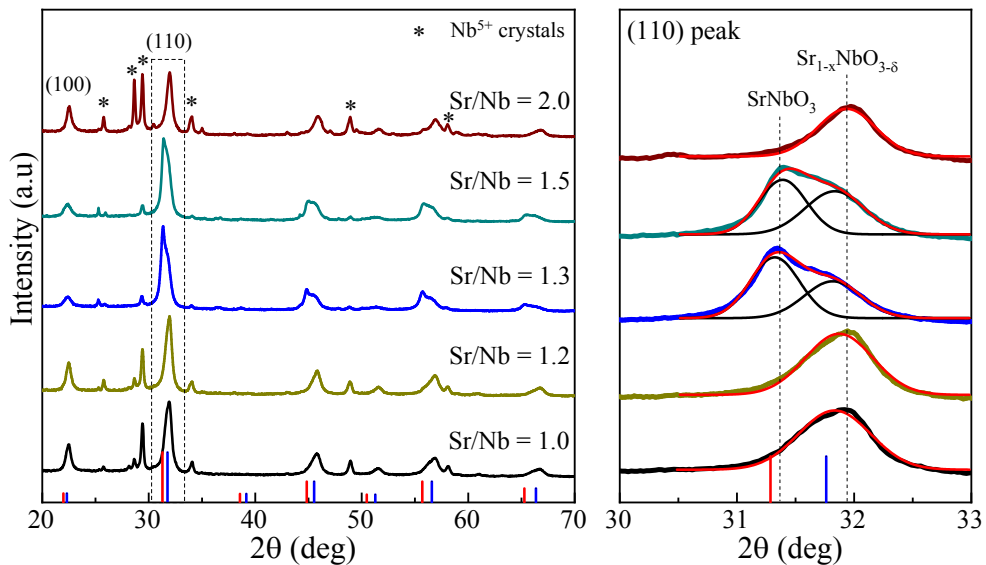


Figure S2. Concentration dependence of $\text{Sr}_{1-x}\text{NbO}_{3-\delta}$ ($\text{Sr}/\text{Nb}=1.0, 1.2, 1.3, 1.5,$ and 2.0) diffraction pattern (left) and an expanded view (right) of the diffraction pattern from $2\theta = 30^\circ - 33^\circ$ highlighting change in peak position with increasing Sr concentration. The dashed lines are a guide to the eye for phase identification.

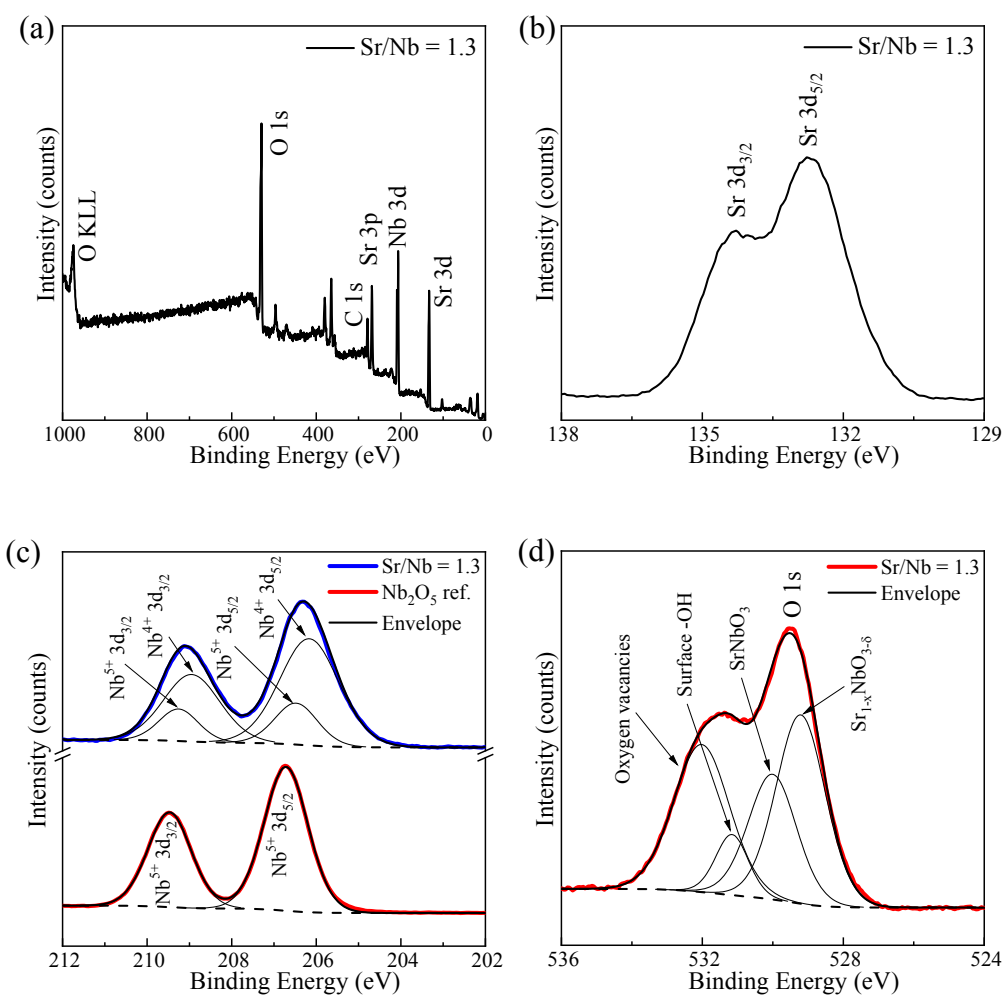


Figure S3. XPS (a) survey scan, (b) Sr 3d spectrum, and (c-d) spectra deconvolution for Nb 3d and O 1s in Sr_{1-x}Nb_xO_{3.6} (Sr/Nb=1.3) nanoparticles synthesized under total pressure of 0.2 Torr. Nb 3d scan shows two visible oxidation states for niobium, Nb⁵⁺ (minority species, ~23%) and Nb⁴⁺ (majority species, ~77%). Peaks due to lattice oxygens (SrNbO₃, Sr_{0.7}NbO_{3.6}), surface hydroxyl groups, and oxygen vacancies are visible in the O 1s scan.

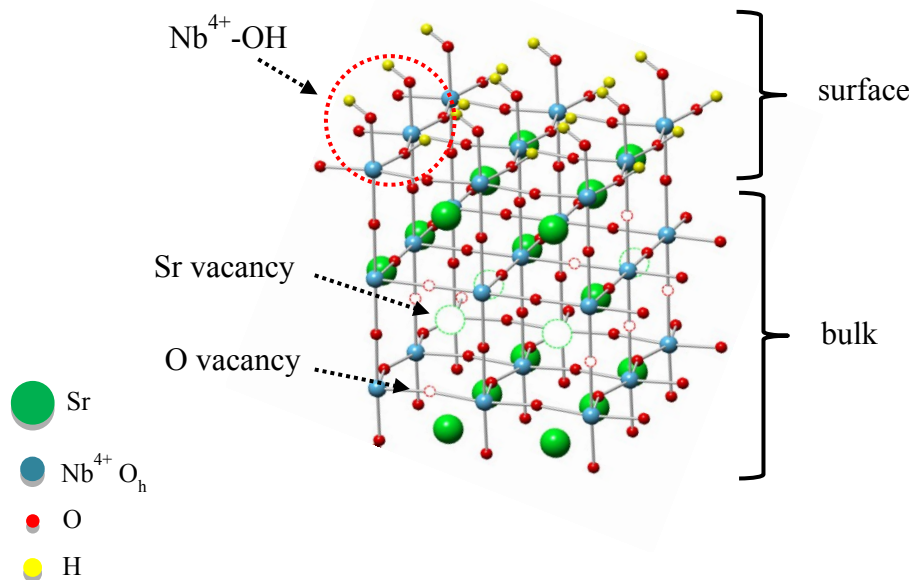


Figure S4. Schematic representation of the $\text{Sr}_{1-x}\text{NbO}_3$ crystal. The model is presented in ball and stick form to highlight the presence of $\text{Nb}^{4+}\text{-OH}$ groups on the surface and point defects (Sr and O vacancies) in the bulk of the nanoparticle.

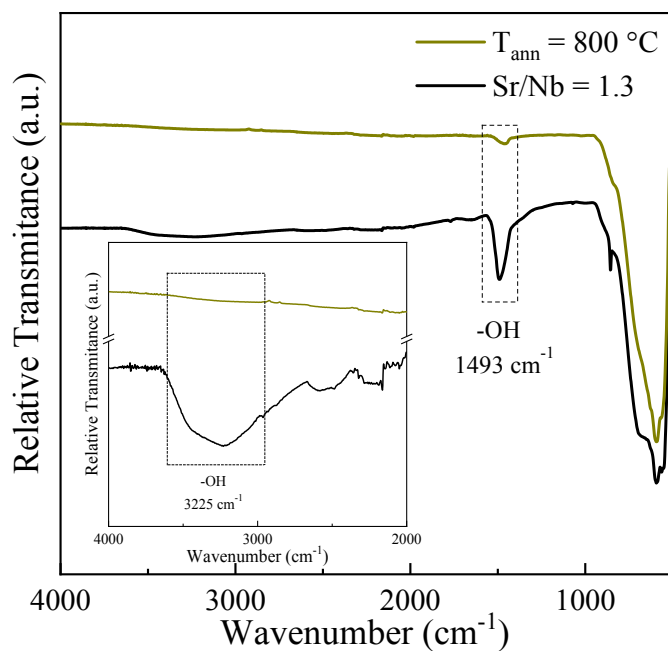


Figure S5. FTIR spectra for as-synthesized and H_2/Ar annealed $\text{Sr}_{1-x}\text{NbO}_{3-\delta}$ ($\text{Sr/Nb}=1.3$) NPs. The peaks ascribed to hydroxyl groups, positioned at 1493 and 3225 (inset) cm^{-1} , are significantly reduced after the annealing process.

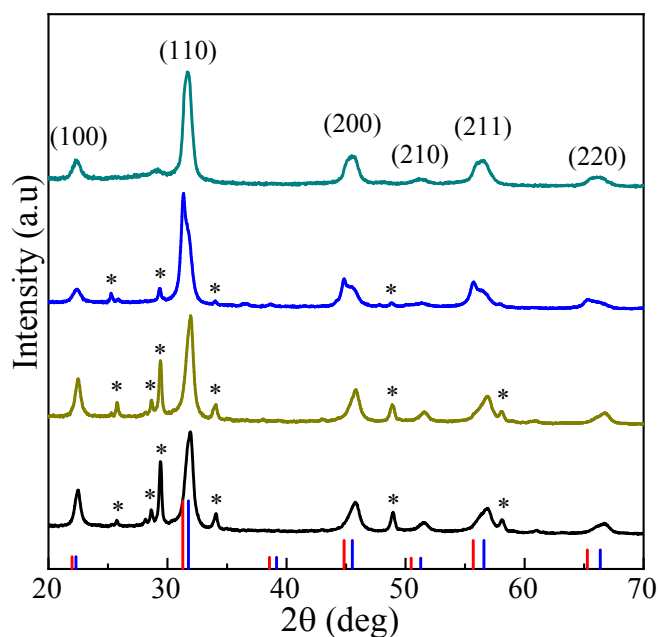


Figure S6. Diffraction patterns for as-synthesized $\text{Sr}_{1-x}\text{NbO}_{3-\delta}$ ($\text{Sr}/\text{Nb}=1.0, 1.2,$ and 1.3) and H_2/Ar annealed $\text{Sr}_{1-x}\text{NbO}_{3-\delta}$ ($\text{Sr}/\text{Nb}=1.3$) NPs. The diffraction patterns highlight the absence of the Nb^{5+} crystals after the H_2/Ar annealing process.

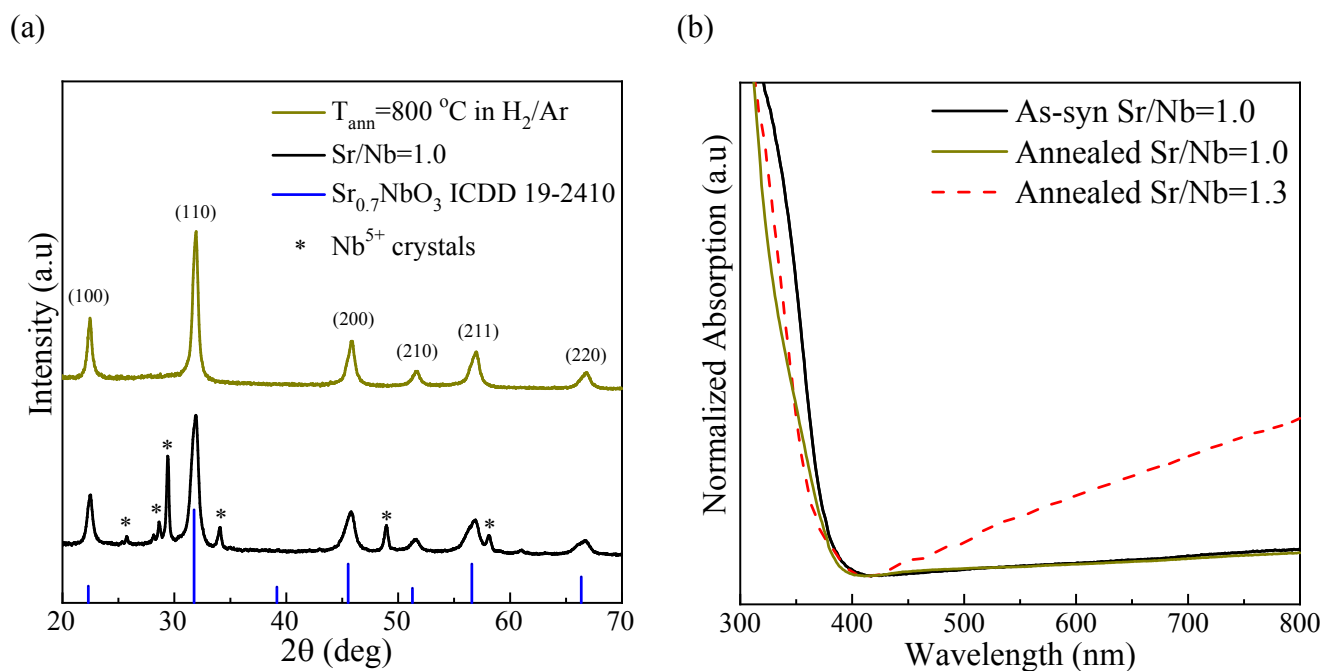


Figure S7. (a) Diffraction patterns and (b) optical absorption spectra for as-synthesized and H_2/Ar annealed $\text{Sr}_{1-x}\text{NbO}_{3-\delta}$ ($\text{Sr}/\text{Nb}=1.0$) NPs. The diffraction patterns highlight the absence of the Nb^{5+} crystals and the absorption spectra show no significant change in the absorption after the annealing process.

Tables

Table S1. ICP-OES Analysis on Sr/Nb=1.3

Sr/Nb = 1.3 Sample	ICP-OES (mg/L)	ICP-OES (mmol/L)	ICP-OES (mol%)	SrNbO ₃ / Sr _{0.7} NbO ₃ (mol%)
Trial #1	Sr (2.235) Nb (2.476)	Sr (0.026) Nb (0.027)	Sr (49%) Nb (51%)	Sr (46%) Nb (54%)
Trial #2	Sr (2.480) Nb (2.750)	Sr (0.028) Nb (0.030)	Sr (49%) Nb (51%)	-
Trial #3	Sr (2.676) Nb (2.967)	Sr (0.031) Nb (0.032)	Sr (49%) Nb (51%)	-
Average	Sr (2.464±0.221) Nb (2.731±0.250)	Sr (0.028±0.003) Nb (0.029±0.003)	Sr (49%) Nb (51%)	-

Table S2. Refined Atomic

Coordinates and Structural

Parameters at Room

Temperature for Sr/Nb=1.3

based on X-ray Diffraction

Parameters	SrNbO ₃	Sr _{0.7} NbO ₃
Atomic Coordinates		
Sr (x,y,z)	0, 0, 0	1/2, 1/2, 1/2
Nb (x,y,z)	1/2, 1/2, 1/2	0, 0, 0
O (x,y,z)	0, 1/2, 1/2	1/2, 0, 0
Structural Parameters		
Sr-O (Å)	2.858(7)	2.816(2)
Nb-O (Å)	2.021(4)	1.991(4)
O-Nb-O (deg)	180	180
O-Nb-O (deg)	90	90
Nb-O-Nb (deg)	180	180

Data.

The occupancy was fixed to 1 at all atom sites for the SrNbO₃ structure and to 0.7 at the Sr site and 1 at Nb and O sites for the Sr_{0.7}NbO₃ structure. For the SrNbO₃, the isotropic displacement parameter U_{iso} is 0.036(2), 0.002(9), and 0.045(1) Å² for Sr, Nb, and O sites, respectively. For the Sr_{0.7}NbO₃, the isotropic displacement parameter U_{iso} is 0.016(4), 0.005(5), and 0.001(8) Å² for Sr, Nb, and O sites, respectively.

Table S3. Detailed Calculation for δ based on Rietveld Refinement and O 1s XPS Spectrum for Sr/Nb=1.3.

Phase	O 1s XPS		Rietveld Refinement		Oxygen Vacancy	
	Peak Area	Area Ratio	Peak Area	Area Ratio	Peak Area	Area Ratio
Stoichiometric	35,859.54	0.61	35,859.54	0.50	-	-
Sr-deficient	23,308.70	0.39	35,841.99	0.50	12,533.29	0.35
Total	59,168.24		71,701.53			

Table S4. Comparison of SNO (Sr/Nb=1.3) Raman Spectrum and Experimental SrTiO₃ Frequencies.

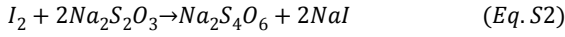
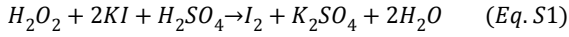
Phonon Branch	Symmetry	Experimental Frequency (cm ⁻¹)	Published work on SrTiO ₃ (cm ⁻¹) ^{a,b}
TO ₁	F _{1u}	129	118
LO ₁	F _{1u}	138	175
TO ₂	F _{1u}	260	185
LO ₂	F _{1u}	433	475
TO ₄	F _{1u}	556	550
LO ₄	F _{1u}	821	795

^{a,b} Experimental Raman scattering data from refs 66 and 67

Iodometric Titration Calculation

Standardization of Na₂S₂O₃ solution

Prepare 30 mL of 0.04 M H₂O₂ (1.2 mmol) which yields 2.4 mmol of Na₂S₂O₃ (equation S1 and S2). From the titration, 31 mL of Na₂S₂O₃ is utilized. Therefore, the actual concentration of Na₂S₂O₃ is 0.08 M.



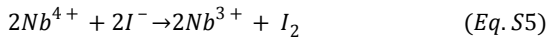
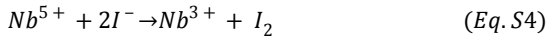
Oxygen Vacancy Calculation from Na₂S₂O₃ titration

The oxygen vacancy is calculated based on a recent report¹ and adapted as followed with the chemical formula for the Sr-deficient phase, from Rietveld analysis, determined as: $Sr_{0.7}^{2+} Nb_{(1-\alpha-\beta)}^{4+} Nb_{\alpha}^{5+} Nb_{\beta}^{3+} O_{3-\delta}$

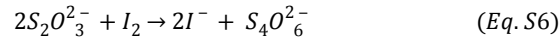
Applying charge neutrality conditions to correlate δ to α and β :

$$\delta = 0.3 - \frac{1}{2}\alpha + \frac{1}{2}\beta \quad (Eq. S3)$$

Dissolving sample in HNO₃ and reacting with KI:



Reaction for Iodine titration with a standard Na₂S₂O₃ solution:



Concentration of formed I₂: from the titration, where C is the concentration (mmol/mL) and V is the volume (mL) of the Na₂S₂O₃ solution:

$$[I_2] = [Nb^{5+}] + 0.5[Nb^{4+}] \quad (Eq. S7)$$

$$[I_2] = \frac{1}{2}CV \quad (Eq. S8)$$

Molar mass of Sr_{0.7}NbO_{3- δ} (M) is a function of the molar mass of Sr_{0.7}NbO₃ (M_o , 228.53 mg/mmol), oxygen (m_1 , 16 mg/mmol), and δ :

$$M = M_o - m_1\delta \quad (Eq. S9)$$

Rewriting equation S5 in terms of α and β and combining with S6, m is the mass of Sr_{0.7}NbO_{3- δ} sample:

$$\frac{1}{2}CV = \alpha\left(\frac{m}{M}\right) + 0.5(1-\alpha-\beta)\left(\frac{m}{M}\right) \quad (Eq. S10)$$

Substituting equation S3 and S9 into S10:

$$\frac{1}{2}CV = (0.8 - \delta)\left(\frac{m}{M_o - m_1\delta}\right) \quad (Eq. S11)$$

Finally, solving for δ from equation S11:

$$\delta = \left(\frac{M_o CV - 1.6m}{m_1 CV - 2m}\right)$$

The blank experiment shows slight I₂ formation due to the presence of atmospheric oxygen. Therefore, to eliminate atmospheric contribution 0.1 mL (or 0.008 mmol) was subtracted from the final titration volumes of Trial 1-3 and displayed in Table S5. The oxygen non-stoichiometry is calculated using $m = 9$ mg and $C = 0.08$ M (from above).

Table S5. Titration Results

Experiment	Volume Na ₂ S ₂ O ₃ (V, mL)	Mole Na ₂ S ₂ O ₃ (CV, mmol)	δ
Blank	0.100	0.008	-
Trial #1	0.500	0.040	0.30
Trial #2	0.400	0.032	0.41
Trial #3	0.400	0.032	0.41
Average	0.433±0.058	0.035±0.005	0.37±0.06

References

1. Y. Wang, L. Chen, H. Cao, Z. Chi, C. Chen, X. Duan, Y. Xie, F. Qi, W. Song and J. Liu, *Appl. Catal. B*, 2019, **245**, 546-554.